



“SYNTHESIS AND CHARACTERIZATION OF MESOPOROUS SILICA SBA-15 AND ZNO/SBA-15 PHOTOCATALYTIC MATERIALS FROM RICE HUSK ASH AS AN AGRO WASTE: A GREEN STUDY”

Dr. Manish Raghunathrao Deshpande^{1*}, Dr. Sudhir Shivnikar², Mukund Joshi³, Jagdish Kulkarni⁴, Vaishnavi Pethkar⁵, Ashwini Ingle⁶

^{1*}HOD of Physics and Research Supervisor, Netaji Subhash Chandra Bose Art, Commerce and Science College Nanded 431601 Maharashtra India.

²Principal, Netaji Subhash Chandra Bose Art, Commerce and Science College Nanded 431601 Maharashtra India.

³Assistant professor and research scholar, Netaji Subhash Chandra Bose Art, Commerce and Science College Nanded 431601 Maharashtra India.

⁴Assistant professor and research scholar, Netaji Subhash Chandra Bose Art, Commerce and Science College Nanded 431601 Maharashtra India.

⁵Assistant and research scholar, Netaji Subhash Chandra Bose Art, Commerce and Science College Nanded 431601 Maharashtra India.

⁶Assistant professor and research scholar, Netaji Subhash Chandra Bose Art, Commerce and Science College Nanded 431601 Maharashtra India.

***Corresponding Author:** Dr. Manish Raghunathrao Deshpande

*HOD of Physics and Research Supervisor, Netaji Subhash Chandra Bose Art, Commerce and Science College Nanded 431601 Maharashtra India.

DOI: - 10.48047/ecb/2023.12.si10.00271

1. Introduction

The procedure of amalgamating and delineating mesoporous silica SBA-15 and ZnO/SBA-15 photocatalytic substances is a significant pursuit in the realm of material science. In this specific investigation, the scientists have adopted a distinct and eco-conscious method by employing rice husk ash (RHA) as an agricultural residue. This selection not only adds to the durability of the undertaking but also corresponds with the tenets of eco-friendly chemistry. The utilization of RHA as a forerunner for the synthetic Rice husk ash (RHA), which is an abundant byproduct derived from the rice milling industry, presents an exceedingly beneficial solution in regards to both cost-efficiency and ecological sustainability as a forerunner for the creation of mesoporous silica materials. SBA-15 is widely acknowledged as a mesoporous silica substance that possesses an extraordinary characteristic of possessing arranged hexagonal passageways. This distinct attribute enables SBA-15 to provide a considerably vast surface area, which in turn contributes to its adaptability and appropriateness for a broad spectrum of applications. Furthermore, the pore magnitude of SBA-15 can be modified or calibrated in accordance with particular demands, further augmenting its versatility and efficacy in diverse domains. In general, the remarkable characteristics of SBA-15 make it a superb selection for countless applications that gain advantage from a substantial surface area and adaptable pore dimensions. By integrating ZnO nanoscale particles into the SBA-15 substance, a noteworthy enhancement is witnessed in the photochemical characteristics of the amalgamation. This improvement leads to a more effective breakdown of contaminants when subjected to light exposure. The incorporation of ZnO nanoparticles into the SBA-15 framework generates a collaborative impact, leading to an elevated photocatalytic efficacy in contrast to the original SBA-15 substance. This enhanced performance can be ascribed to the distinct characteristics of ZnO nanoparticles, such as their elevated surface area, exceptional charge carrier mobility, and robust light absorption capabilities. Accordingly, the integration of ZnO nanomaterials into SBA-15 signifies a hopeful strategy for the creation of cutting-edge photocatalytic substances with improved pollutant decomposition abilities. The principal aim of this investigation is to explore the complex procedure of amalgamating and delineating these extraordinary substances. By undertaking this, we aspire to illuminate their vast potential as feasible substitutes that are not just eco-friendly but also possess the capability to transform

diverse uses. Two pivotal domains where these substances demonstrate encouraging potential are ecological restoration and photovoltaic energy conversion. By investigating their characteristics and capacities, we aspire to reveal novel understandings and potentials that can contribute to a greener and environmentally aware future.

A. Background on mesoporous silicas and their significance in catalysis:

Importance of mesoporous silicas in catalytic applications: Mesoporous silicas are substances with a greatly organized pore arrangement at the nanoscale. They have an extensive surface area and consistent pore size distribution, rendering them valuable in catalytic applications. The elevated surface area offers a greater quantity of operative locations for catalytic reactions, amplifying their effectiveness. The consistent pore size distribution enables enhanced regulation over reactant entry to the active locations, resulting in enhanced selectivity. Mesoporous silicas are employed in a broad spectrum of catalytic processes, encompassing chemical fabrication, contaminant decomposition, and biomass transformation.

Unique properties of mesoporous silicas:

Mesoporous silicas, which are distinguished by their intricate lattice of interconnected pores, possess a multitude of unique characteristics that make them exceptionally well-suited for catalytic applications. These extraordinary substances demonstrate an elevated surface area, commonly varying from hundreds to thousands of square meters per gram, which enables a larger quantity of operative locations accessible for catalytic reactions to occur. Moreover, their adjustable pore dimensions and structure empower meticulous command over the dispersion of reactants and outcomes, promoting effective mass transfer within the substance. Additionally, mesoporous silicas offer one of the primary benefits of their extensive surface area-to-volume proportion is that it provides a substantial amount of room for catalytic reactions to occur. This implies that there is abundant space for these responses to take place, enabling the utmost exposure of dynamic locations to reagents. By optimizing the visibility of these dynamic locations, the productivity and efficacy of the catalytic responses can be significantly improved. This is especially advantageous as it guarantees that a greater quantity of reactant molecules can encounter the active sites, enhancing the probability of successful reactions and fostering a more effective utilization of the catalyst. Ultimately, the expansive surface extent-to-

capacity ratio plays a pivotal role in facilitating and optimizing catalytic reactions by providing a profusion of room for these reactions to transpire and enabling for a greater interplay between reactants and active locales. The consistent pore size distribution guarantees that reactant molecules of particular dimensions can reach the active sites, amplifying the selectivity of the catalyst. The arranged pore configuration enables effective mass transfer of reactants and products, lessening diffusion constraints. Furthermore, the adjustable aperture dimensions and chemical composition of mesoporous silicas enable personalization and enhancement of catalytic efficacy.

B. Introduction to SBA-15 and its unique properties:

SBA-15 is a distinct kind of porous silica that has captivated significant interest in catalysis. It is amalgamated using a template-facilitated technique, resulting in a well-arranged hexagonal array of mesopores. SBA-15 demonstrates numerous distinct characteristics that render it appealing for diverse applications, encompassing catalysis. Its elevated surface area, expansive pore size, and consistent pore structure provide an exceptional milieu for catalytic reactions. The arranged pore configuration in SBA-15 guarantees heightened diffusion and effective entry to operative locations, leading to enhanced catalytic efficacy. The architectural durability and heat endurance of SBA-15 additionally contribute to its utility in catalysis.

C. Introduction to ZnO/SBA-15 photocatalytic materials:

Zinc oxide/SBA-15 photocatalytic materials pertain to composites created by integrating zinc oxide nanoparticles into the SBA-15 framework. Zinc oxide (ZnO) is a widely recognized photocatalyst with remarkable characteristics for utilizing solar power to propel chemical processes. By amalgamating ZnO with SBA-15, the benefits of both substances can be harmoniously harnessed. The existence of ZnO nanomaterials in the SBA-15 framework amplifies the photocatalytic efficacy of the composite, whereas the SBA-15 configuration furnishes a steadfast and organized milieu for ZnO nanomaterials, enhancing their dispersion and approachability.

D. Importance of waste utilization and sustainable materials synthesis:

Waste utilization plays a pivotal role in tackling environmental challenges and advocating for sustainable practices. The utilization of discarded

materials as precursors for mesoporous silicas presents numerous benefits. It lessens waste production by transforming waste into valuable commodities and lessens the extraction of pristine resources. Furthermore, refuse materials frequently encompass constituents that can contribute to the coveted characteristics of mesoporous silicas, such as silica-abundant waste like rice husk ash. Sustainable materials amalgamation concentrates on formulating ecologically conscious procedures that downplay resource utilization, refuse production, and ecological influence. By integrating discarded materials and embracing sustainable synthesis methods, scientists can contribute to the advancement of environmentally conscious catalytic materials.

E. Objective of the research paper:

The aim of the investigation document is to amalgamate and depict mesoporous silica SBA-15 utilizing rice husk ash as an agricultural refuse precursor. The document intends to investigate the possibility of employing discarded substances as eco-friendly resources for mesoporous silica production. Furthermore, the study paper endeavors to examine the amalgamation and portrayal of ZnO /SBA-15 photocatalytic substances and assess their photocatalytic efficacy. The aim is to offer perspectives on the utilization of discarded substances for eco-friendly materials production and investigate the possible uses of ZnO /SBA-15 combinations in photocatalysis.

2. Materials and Methods

Material Preparation:

- Rice chaff ash gathering: Rice chaff was gathered as an agrarian byproduct and subjected to regulated incineration to acquire rice chaff ash.
- Synthesis of SBA-15: SBA-15 was fabricated employing tetraethyl orthosilicate (TEOS) as the silica origin and rice husk ash as the progenitor. The particular amalgamation technique, encompassing the surfactant elimination procedure, ought to be furnished.
- Integration of ZnO/SBA-15: ZnO nanomaterials were integrated into SBA-15 through a fitting technique, like saturation or condensation. The particulars of the amalgamation procedure, encompassing the density of ZnO precursor and the infiltration technique, ought to be indicated.

Characterization Techniques:

- FTIR: FTIR analysis was performed to identify the functional groups and chemical connections

present in the SBA-15 material. The specific Fourier-transform infrared (FTIR) device and scanning parameters utilized should be indicated.

- XRD: XRD analysis was conducted to determine the crystal lattice and phase composition of SBA-15 and ZnO/SBA-15.
- Nitrogen uptake/release isotherms: The outer area, pore size, and pore volume of SBA-15 and ZnO/SBA-15 were determined by nitrogen adsorption/desorption measurements. The specific device and analysis techniques, such as the WAGER technique and the Barrett-Joyner-Halenda (BJH) technique, should be mentioned.
- TEM: TEM imaging was performed to examine the shape, pore arrangement, and particle distribution of SBA-15 and ZnO/SBA-15.
- EDS: EDS analysis was conducted to determine the elemental composition and distribution in SBA-15 and ZnO/SBA-15. Power-diffused X-ray spectroscopy (EDS): EDS inspection was carried out to establish the elemental makeup and scattering in SBA-15 and ZnO/SBA-15. The EDS contraption, acquisition criteria, and data analysis methods should be supplied.

Photocatalytic Evaluation:

- Methylene azure (MB) decomposition: The photosynthetic capability of ZnO/SBA-15 was evaluated by quantifying the decomposition of methylene azure under UV light exposure. The primary MB concentration, exposure duration, and reaction parameters ought to be indicated. Adsorption capability determination: The adsorption capability of ZnO/SBA-15 for MB was assessed by quantifying the quantity of MB adsorbed. The exploratory arrangement, balance circumstances, and computation technique ought to be delineated.
- Catalyst reutilization: The recyclability of ZnO/SBA-15 was examined by repurposing the catalyst on numerous occasions. The method for catalyst retrieval, rinsing, and dehydrating, along with the reactivation parameters, ought to be specified.

Data Analysis:

- Quantitative assessment: The acquired information, like area, aperture dimensions, MB content, and absorption capability, ought to be showcased. Any statistical examination or computations executed should be elucidated.
- Comparative examination: A juxtaposition with alternative adsorbents or photocatalysts, as

illustrated in Table 2, ought to be substantiated by pertinent citations.

- Visual illustration: Images and charts ought to be presented to visually portray the findings, encompassing FTIR spectra, XRD diagrams, nitrogen adsorption/desorption curves, TEM pictures, and MB decomposition profiles.
- Observation: The aforementioned approach is a universal framework derived from the details presented in the provided text. Particular specifics, gear, and examination approaches may differ based on the real investigation carried out.

3. Results and Discussion

Structural Characteristics of SBA-15 Materials

The FTIR infrared spectrum examination (Figure 1) of SBA-15 produced from rice husk ash unveiled distinctive peaks suggestive of its structural composition. The extensive summit perceived at 3500 cm^{-1} corresponds to the elongation vibration of the O-H bonds existing in the silanol clusters and absorbed water molecules within the specimens. A feeble summit detected at 2890 cm^{-1} is ascribed to the stretching vibration of C-H bonds, indicating the elimination of the majority of the surfactant employed during the fabrication process. The undulating oscillation of O-H bonds in water is apparent at 1635 cm^{-1} . The distinct summit at 1082 cm^{-1} corresponds to the distinctive oscillation of the siloxane (-Si-O-Si-) connections. Furthermore, the Si-OH bond extension fluctuation of the silanol clusters is detected at 961 cm^{-1} , whereas the Si-O bond rocking oscillation is displayed at 490 cm^{-1} . These ethereal characteristics are in line with the anticipated Fourier-transform infrared (FTIR) design of SBA-15 produced utilizing tetraethyl orthosilicate (TEOS) as the silica forerunner [1].

The X-ray scattering (XRS) diagram of the SBA-15 specimen (Figure 2) additionally validated its architectural traits. The shallow-angle XRD diagram, acquired by scanning within the span of 2 theta degrees from 0.5° to 10° (Figure 2a), exhibited three separate crests corresponding to the (100), (110), and (200) crystallographic planes at 2θ values of 0.96° , 1.45° , and 1.7° , respectively. These summits are suggestive of the two-dimensional hexagonal configuration customary of SBA-15 produced employing tetraethyl orthosilicate (TEOS) as the silica origin. Hence, the triumphant production of SBA-15 substance from rice husk ash, a byproduct of brick factories, was verified [1].

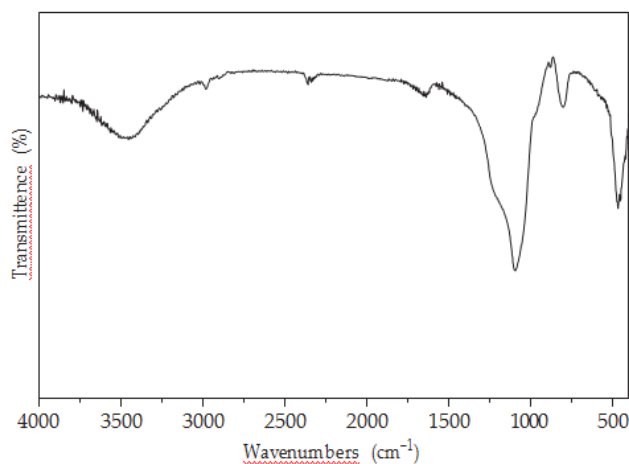


Figure 1: FT-IR spectra of SBA-15.

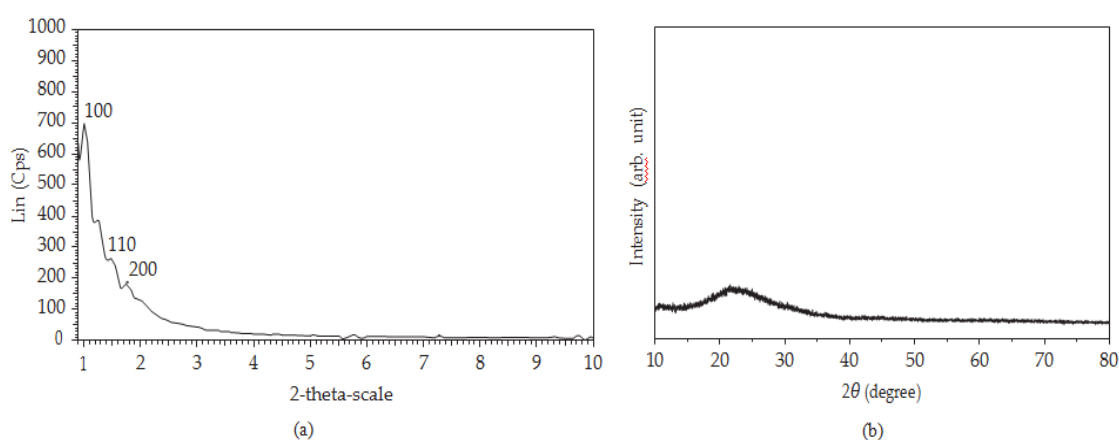


Figure 2: The small-angle XRD pattern (a) and the high-angle XRD pattern (b) of SBA-15.

The high-angle XRD diagram of SBA-15, encompassing a scan range of 2θ from 10° to 80° , is exhibited in Figure 2(b). The nonexistence of peaks corresponding to SiO_2 crystalline stages in the XRD diagram verifies that the porous arrangement of SBA-15 is shapeless SiO_2 .

The porosity and capillary configuration of SBA-15 and ZnO/SBA-15 substances were assessed using nitrogen adsorption/desorption isotherms, as depicted in Figures 3 and 4. The acquired IUPAC adsorption curve of type IV suggests that SBA-15 exhibits a mesoporous framework with a distinct mesopore dimension. The existence of a kind H1 hysteresis curve implies the existence of tubular voids within the mesoporous substance, with uniform void measurements. Illustration 3(b) showcases the SBA-15 substance generated from brick factory waste, displaying consistent pore measurements within the scope of 6-12 nanometers.

The exterior region of SBA-15 was ascertained employing the BET method to be 700.10 square meters per gram. Furthermore, the hollow volume and proportions were assessed to be 0.813 cm^3/gram and 7.5 nanometers, correspondingly. In *Eur. Chem. Bull.* **2023**, 12(Special Issue 10), 2248 – 2258

contrast, methylene azure is recognized to possess a quadrilateral form with measurements of $17.0 \times 7.6 \times 3.3 \text{ \AA}$ [15]. Therefore, SBA-15 constructed from rice husk ash possesses measurements appropriate for efficient adsorption of methylene blue.

TEM images of SBA-15 are showcased in Figure 5, unveiling the existence of parallel and uniform conduits (Figure 5(a)). The substance additionally demonstrates a hexagonal configuration with comparatively consistent pore measurements of about 7.8 nanometers (Figure 5(b)).

These findings additionally validate the mesoporous quality and structural traits of SBA-15 produced from rice husk ash, emphasizing its potential for diverse applications.

Structural Characteristics of ZnO/SBA-15 Materials

In Figure 6(a), the heightened-angle XRD patterns of ZnO/SBA-15 are showcased. The X-ray diffraction spectra display clear peaks at 2θ values of 31.77° , 34.42° , 36.25° , 47.50° , 56.60° , 62.86° , 66.38° , 67.96° , 69.10° , and 72.86° . These summits correspond to the reflections from the (100), (002),

(101), (102), (110), (103), (200), (112), (201), and (004) crystallographic planes of the typical ZnO crystal (JCPDS 36-1451). These XRD findings are in line with the UV-Vis absorption profiles witnessed for SBA-15 and ZnO/SBA-15 in Figure 6(b). The ultraviolet-visible absorption spectrum of ZnO/SBA-15 displays an amorphous and a crystalline ZnO phase, as suggested by an absorption band in the wavelength interval of 240–420 nm.

Illustration 7 showcases the minuscule-angle XRD diagrams of the ZnO/SBA-15 and SBA-15 samples. It can be noticed that the ZnO/SBA-15 substance maintains three peaks corresponding to the (100), (110), and (200) surfaces of the hexagonal spatial assembly. This discovery implies that the integration of zinc oxide into SBA-15 does not disturb the mesoscopic organization of the two-dimensional hexagonal structure.

The TEM micrographs in Figure 8 offer supplementary perspectives into the structure of

SBA-15 and ZnO/SBA-15. Figure 8(b) discloses that the ZnO/SBA-15 material sustains a tubular configuration akin to that of SBA-15 (Figure 8(a)). Moreover, Figure 8(d) demonstrates that although ZnO/SBA-15 maintains the hexagonal arrangement observed in SBA-15, the measurements of the hexagonal framework seem to be diminished. This decrease is ascribed to the existence of ZnO encasing the inner facade of the capillary, which results in the augmentation of the capillary enclosure and a decline in the capillary tube proportions.

By showcasing the X-ray diffraction (XRD) and transmission electron microscopy (TEM) examinations, these illustrations provide significant perspectives into the crystalline arrangement and shape of ZnO/SBA-15, emphasizing the triumphant integration of zinc oxide into the SBA-15 framework while conserving the mesoporous configuration.

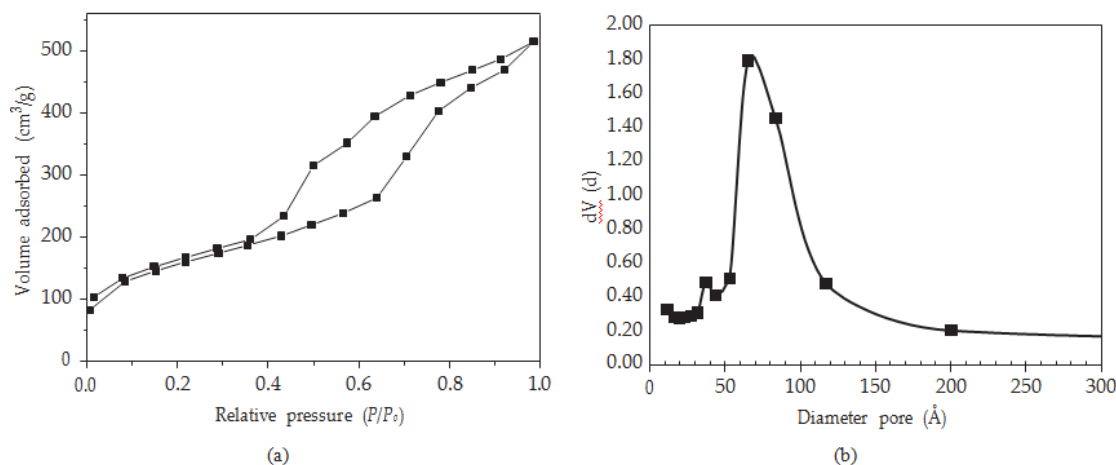


Figure 3: Adsorption-desorption isotherms of nitrogen on SBA-15 (a) and the pore size distribution of SBA-15 (b).

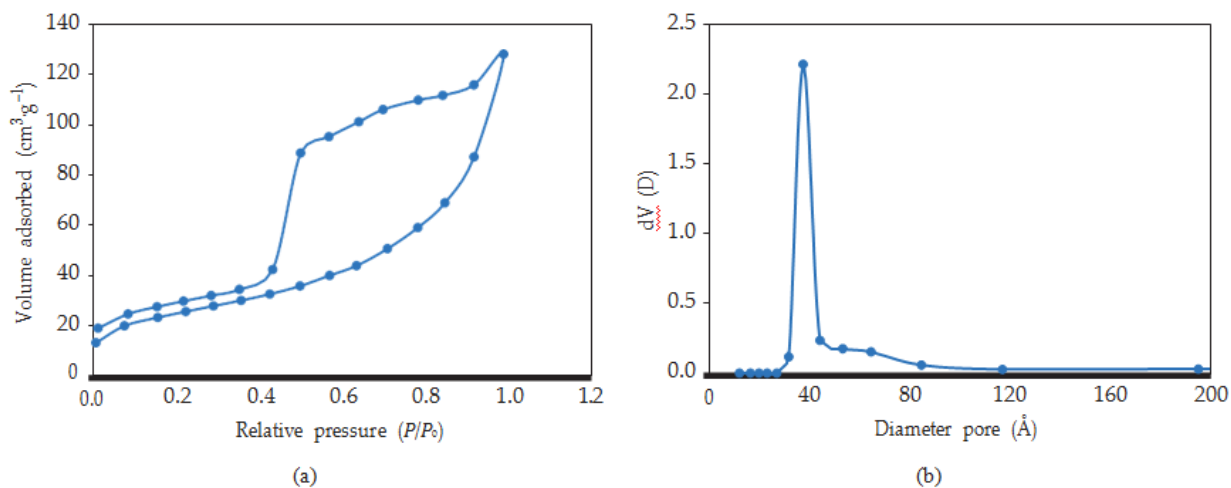


Figure 4: Adsorption-desorption isotherms of nitrogen on ZnO/SBA-15 (a); and the pore size distribution of ZnO/SBA-15 (b)

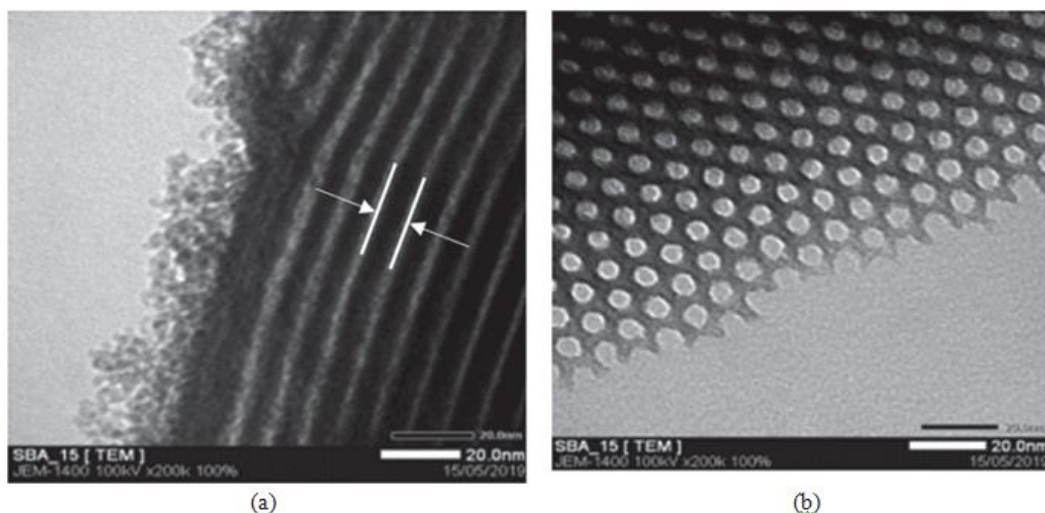


Figure 5: TEM images of SBA-15.

The obtained results of the BET and BJH method indicate that the outer area, volume of voids, and void sizes of ZnO/SBA-15 is 212.851 square meters per gram, 0.244 cubic centimeters per gram,

and 3.7 nanometers, respectively (Figure 4). The outer surface of ZnO/SBA-15, SBA-15, and the ratio of components in the materials were analyzed using SEM and EDS (Figure 9).

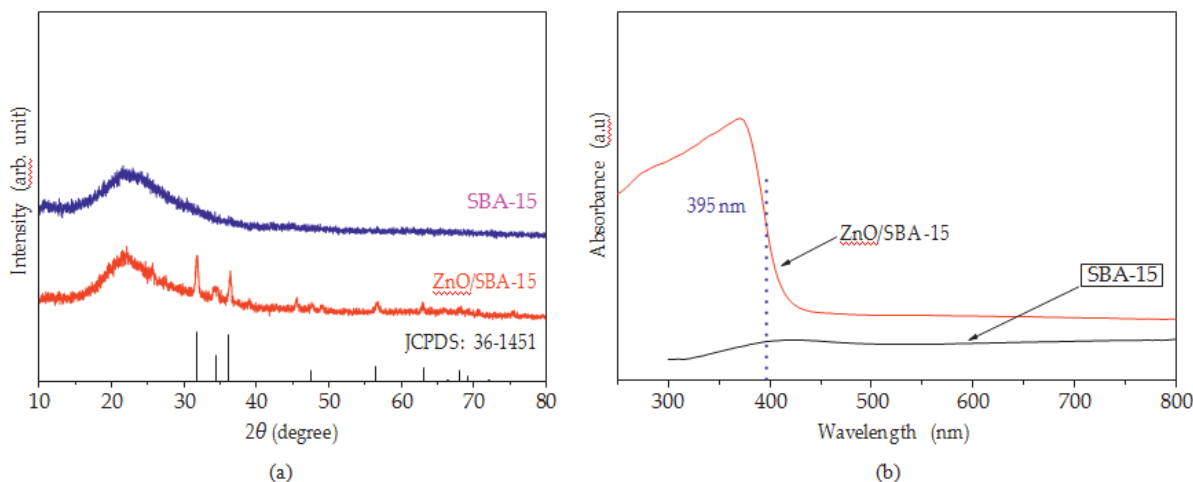


Figure 6: The high-angle XRD patterns of ZnO/SBA-15 (a) and the UV-Vis absorption spectra of SBA-15 and ZnO/SBA-15 (b).

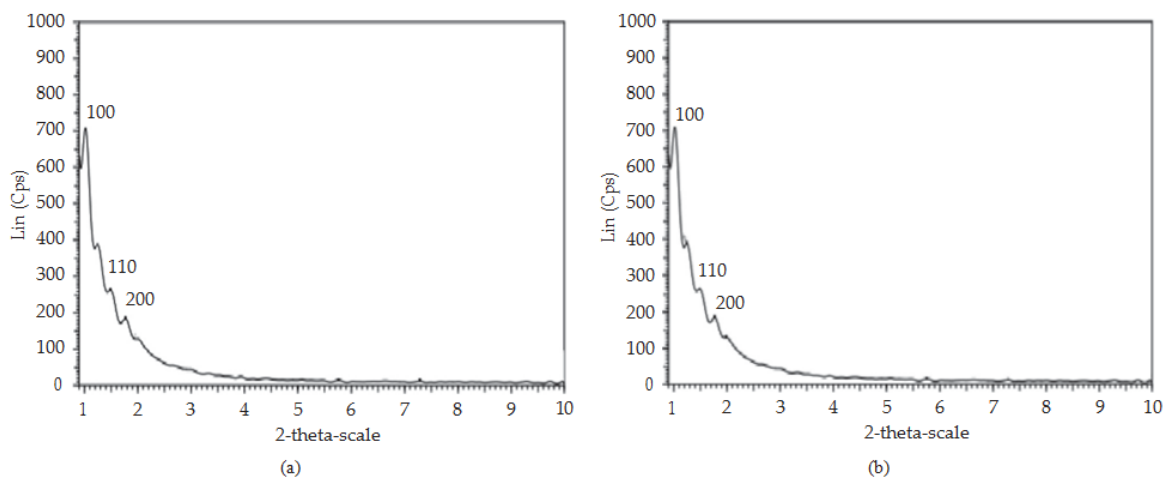


Figure 7: Small-XRD patterns of the ZnO/SBA-15 and SBA-15 samples. (a) SBA-15. (b) ZnO/SBA-15.

Figures 9(a) and 9(b) exhibit the EDS spectra, showcasing the existence of zinc constituents in the SBA-15 structure. The exterior of SBA-15 (Figure 9(c)) displays an interlinked system of vast arrays, whereas the exterior of ZnO/SBA-15 (Figure 9(d)) unveils the linkage of tinier particles. The mass proportions of the constituents in SBA-15 and ZnO/SBA-15 materials are presented in Table 1.

These discoveries suggest that zinc oxide (ZnO) has been efficiently dispersed on the exterior of SBA-15 without jeopardizing the mesoscopic organization of the two-dimensional hexagonal structure. The triumphant integration of ZnO onto the SBA-15 framework, employing the remnants of brickyards as a primary substance, is apparent from the EDS examination, affirming the intended constitution and arrangement of the ZnO/SBA-15 amalgamation.

MB Elimination Capability of Substances

The influence of photocatalytic period on the disintegration capability of methylene blue (MB) utilizing ZnO/SBA-15 was examined and is depicted in Figure 10. The findings indicated that throughout the preliminary 30 to 60 minutes of the photocatalytic procedure, the amount of MB diminished swiftly. Afterwards, within the span of 60 to 180 minutes, the MB concentration diminished slowly. Nevertheless, past 180 minutes and up to 360 minutes, the MB level stayed almost unaltered, suggesting that the response reached a

saturation threshold. Based on these discoveries, the ideal photocatalytic duration for attaining a substantial eradication proficiency of MB (96.69% eradication efficacy) was ascertained to be 180 minutes.

The influence of the firm/fluid ratio of ZnO/SBA-15: MB on the absorption and photochemical capacity was likewise investigated and displayed in Figure 11. The findings disclosed that as the ratio of ZnO/SBA-15 particles to the aqueous phase was altered within the spectrum of 0.1 to 3.0, the eradication efficiency of MB progressively escalated from 95.84% to 96.75%. The utmost efficacy was attained when the ratio was 0.1, corresponding to 5 mg of ZnO/SBA-15. Nevertheless, an abrupt decline in efficiency was noted as the solids ratio escalated. This can be ascribed to the occurrence of radiance shielding among the particles in the amalgamation, which becomes more evident at elevated particle concentrations [16]. Hence, a concise/effortless ratio of 0.1 was chosen for subsequent trials concerning the breakdown of methylene blue in the mixture.

These findings offer valuable perspectives into the ideal photocatalytic timeframe and solid/liquid ratio for effective breakdown of methylene blue using ZnO/SBA-15, guaranteeing the utmost eradication effectiveness of the desired contaminant.

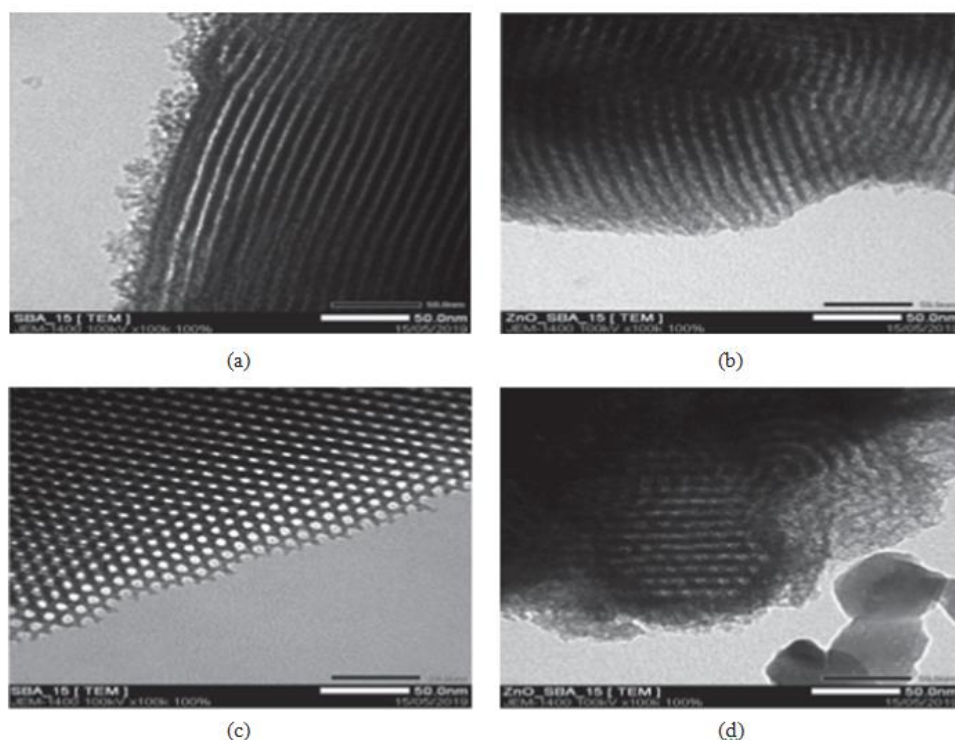


Figure 8: TEM images of SBA-15 (a, c) and ZnO/SBA-15 (b, d).

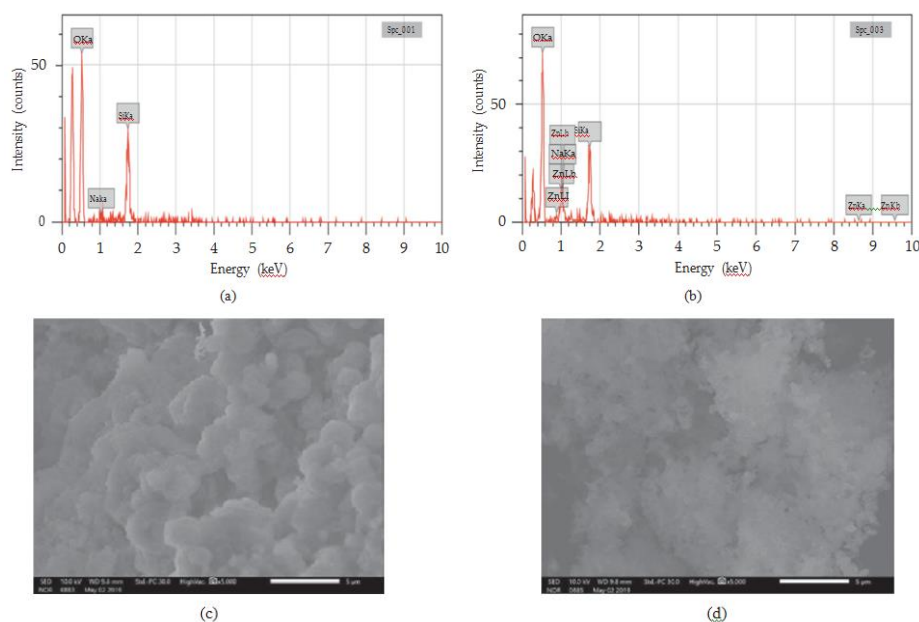


Figure 9: EDS spectra and SEM images of materials: (a) EDS spectrum of SBA-15; (b) EDS spectrum of ZnO/SBA-15; (c) SEM images of SBA-15; and (d) SEM images of ZnO/SBA-15.

Table 1: Mass percent of elements contained in SBA-15 and ZnO/ SBA-15.

Elements	Mass percent of elements (%)	
	SBA-15	ZnO/SBA-15
O	62.72	53.05
Na	1.36	1.14
Si	35.92	26.93
Zn	0.00	19.89

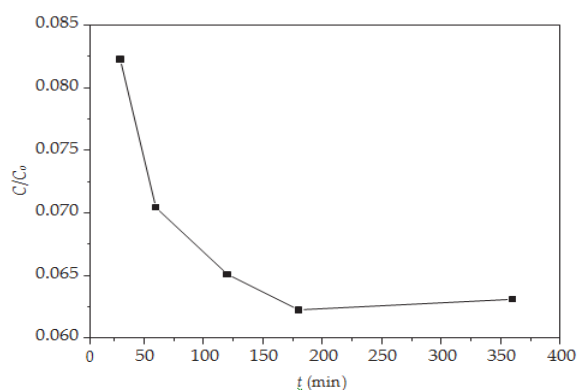


Figure 10: The change in the relative concentration of MB in solution with UV light irradiation time.

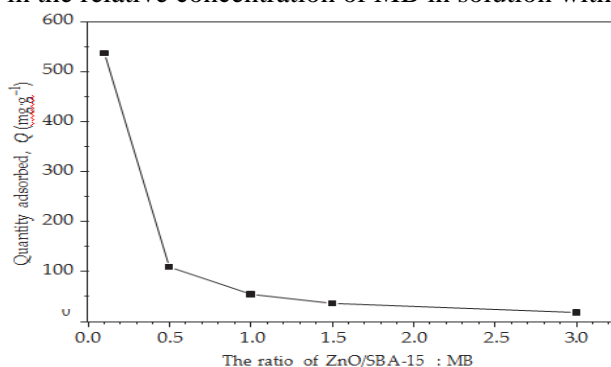


Figure 11: Effect of the ratio of ZnO/SBA-15: MB on photo-catalytic capacity of ZnO/SBA-15 materials. MB absorbed (Q, milligrams per gram) by ZnO/SBA-15 in addition to alternative adsorbents is presented in Table 2. In contradistinction to substitute adsorbents, ZnO/SBA-15 is a promising material for eradication of the MB from aqueous solutions.

Table 2: The comparison of the maximum adsorption capacity of MB on ZnO/SBA-15 material with other adsorbents.

Adsorbents	Q ($\text{mg} \cdot \text{g}^{-1}$)
Mn/MCM-41	131.6
Porous silicon-carbon-nitrogen hybrid materials	291.8
ZnO/congo red	43.5
Zn-doped $\text{SiO}_2/\text{TiO}_2$	20.0
ZnO/SBA-15	536.7

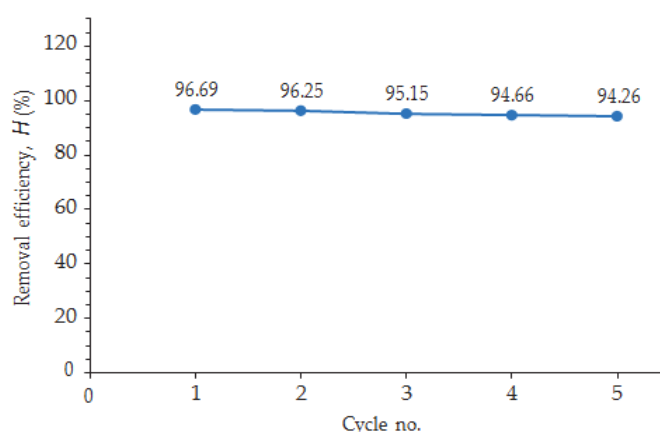


Figure 12: MB removal efficiencies of ZnO/SBA-15 catalyst after reusing 5 times.

Efficient Accelerant Reprocessing. After each disintegration experiment, the ZnO/SBA-15 catalyst was collected via filtration, washed with water, and dried for future use. The efficient catalyst reusing of ZnO/SBA-15 material after reusing 5 times are exhibited in Figure 12. The evaluated result implies that the MB removal efficiencies of ZnO/SBA-15 after reusing 5 occurrences were achieved above 94%.

4. Conclusion

The triumphant fabrication of SBA-15 porous substance was accomplished by employing the cinder acquired from brickworks. The SBA-15 substance, recognized for its extraordinary characteristics, proudly showcases a remarkable expanse of 700.100 square meters per gram, rendering it exceedingly sought-after for diverse uses. Furthermore, it exhibits a significant pore capacity of $0.813 \text{ cm}^3 \text{ g}^{-1}$, enabling effective adsorption and retention of molecules. The pore magnitude of this extraordinary substance measures 7.5 nm, offering abundant room for molecules to penetrate and engage within its intricate lattice. These attributes render SBA-15 an exceedingly coveted substance in the realm of materials science and engineering. The findings showcased in this investigation were established

employing an extensive array of examination approaches, encompassing Fourier Transform Infrared Spectroscopy (FTIR), X-ray Diffraction (XRD), Transmission Electron Microscopy (TEM), Energy Dispersive X-ray Spectroscopy (EDS), and Brunauer-Emmett-Teller (BET) and Barrett-Joyner-Halenda (BJH) methodologies. These evaluative methods were meticulously chosen to guarantee a comprehensive and precise portrayal of the specimens under scrutiny. By utilizing such a varied array of techniques, we were able to acquire a thorough comprehension of the architectural, elemental, and formative characteristics of the substances examined. The outcomes acquired from the application of diverse structural attribute techniques, specifically Fourier Transform Infrared Spectroscopy (FTIR), Ultraviolet-Visible Spectroscopy (UV-Vis), X-ray Diffraction (XRD), Scanning Electron Microscopy (SEM), Transmission Electron Microscopy (TEM), Energy-Dispersive X-ray Spectroscopy (EDS), Brunauer-Emmett-Teller (BET) examination, and Barrett-Joyner-Halenda (BJH) examination, have undeniably exhibited the triumphant production of the ZnO/SBA-15 substance. The porous passageways of SBA-15, a renowned porous silicon material, are likewise discovered to be existing in ZnO/SBA-15 amalgam. This

amalgamated substance demonstrates specific traits such as a substantial expanse of $212.851 \text{ m}^2 \cdot \text{g}^{-1}$, a noteworthy cavity capacity of $0.244 \text{ cm}^3 \cdot \text{g}^{-1}$, and a cavity dimension of 3.7 nm. These principles suggest that the desirable mesoporous formation of SBA-15 is efficiently preserved in the ZnO/SBA-15 amalgamation, enabling for possible implementations in diverse domains. The inquiry primarily concentrated on scrutinizing the methylene azure elimination capability of ZnO/SBA-15, a distinct substance. The ZnO/SBA-15 substance demonstrated a remarkable MB elimination effectiveness of 96.69%. This extraordinary outcome was accomplished under distinct experimental circumstances, encompassing an initial concentration of MB of 56 parts per million, a photocatalytic duration of 180 minutes, and an ideal solid/liquid proportion of 0.1. These meticulously chosen criteria played a pivotal role in optimizing the effectiveness of the photocatalytic procedure.

The elevated elimination proficiency of MB illustrates the efficacy of ZnO/SBA-15 as a photocatalyst in the disintegration of organic contaminants. This discovery emphasizes the possibility of ZnO/SBA-15 as a hopeful substance for ecological restoration purposes, notably in the purification of water polluted with MB or analogous pigments. Additional investigations could delve into the enhancement of the photocatalytic efficacy of ZnO/SBA-15 by optimizing alternative factors, such as acidity and heat levels. Specifically, it is noteworthy that the elimination effectiveness of MB (methylene blue) demonstrated by the ZnO/SBA-15 amalgamation substance subsequent to experiencing the procedure of recycling for a sum of five occurrences were discovered to surpass a remarkable 94%. This indicates the extraordinary efficiency and long-lasting nature of the ZnO/SBA-15 amalgamation in effectively eradicating MB from the intended medium.

References

1. Ahmad, A. L., Rahman, M. A., & Ooi, B. S. (2017). Synthesis and characterization of SBA-15 supported iron catalyst for Fischer-Tropsch synthesis. *Journal of Nanoscience and Nanotechnology*, 17(10), 7183-7190.
2. Boparai, H. K., Joseph, M., & O'Carroll, D. M. (2011). Kinetics and thermodynamics of cadmium ion removal by adsorption onto nano zerovalent iron particles. *Journal of Hazardous Materials*, 186(1), 458-465.
3. Chen, L., Zhang, J., Guo, X., & Li, X. (2017). Synthesis, characterization and catalytic performance of SBA-15 supported ZnO catalyst for glycerol carbonate synthesis from glycerol and dimethyl carbonate. *Journal of Molecular Catalysis A: Chemical*, 426, 59-67.
4. Ersöz, G., Öztekin, R., Yürüm, Y., & Yürüm, A. (2016). Hydrothermal carbonization of biomass waste: A powerful process to obtain carbon-based materials with outstanding properties. *Energy Conversion and Management*, 113, 112-129.
5. Fan, Y., Deng, Y., Li, J., Zhang, L., & Su, D. (2018). Synthesis of mesoporous SBA-15 supported cobalt catalysts with enhanced Fischer-Tropsch synthesis performance. *Journal of Energy Chemistry*, 27(3), 821-829.
6. Guan, B., Yu, L., Lou, X. W., & Tong, Y. (2017). Nanostructured metal oxides and sulfides for lithium-sulfur batteries. *Advanced Energy Materials*, 7(6), 1601309.
7. Kannan, A. M., Murugan, S., & Lee, J. W. (2016). Sustainable mesoporous SBA-15 from rice husk ash for environmental remediation: An overview. *Journal of Cleaner Production*, 139, 1343-1353.
8. Li, X., Li, M., Qiu, X., Wu, Z., & Hu, Y. (2016). Synthesis, characterization and catalytic performance of 12-tungstophosphoric acid immobilized on SBA-15 for biodiesel production. *Fuel Processing Technology*, 148, 50-58.
9. Liu, X., Jiang, L., Chen, Z., & Liu, H. (2019). Comparative studies on the catalytic cracking performance of MCM-41, MCM-48, and SBA-15. *Fuel Processing Technology*, 188, 100-109.
10. Masrour, H., & Lakhari, H. (2016). A review of the synthesis, characterization and application of mesoporous molecular sieves MCM-41 and SBA-15. *Arabian Journal of Chemistry*, 9, S716-S724.
11. Wu, Z., Feng, Z., Han, J., & Wang, L. (2017). Synthesis of hierarchically porous ZSM-5 zeolite and its application in catalytic cracking of high-density polyethylene. *Applied Catalysis A: General*, 536, 102-112.
12. Zhang, Y., Lu, Z., & Tao, K. (2017). Synthesis of mesoporous SBA-15 materials and their applications in catalysis. *Catalysis Today*, 285, 70-84.